JOURNAL OF THERMOPHYSICS AND HEAT TRANSFER
Vol. 11, No. 1, January–March 1997

Numerical Investigation of Vibrational Nonequilibrium Effects in Hydrogen–Oxygen Rocket Engines

Richard A. Jones,* Leik N. Myrabo,† and Henry T. Nagamatsu‡
Rensselaer Polytechnic Institute, Troy, New York 12180

A computational method has been developed to simulate gas nozzle flows expanding in vibrational nonequilibrium. Comparisons of the effect of nonequilibrium on flowfield variables are made with available experimental data. Several experimental investigations of expanding nitrogen flowfields are simulated and compared. Significant changes in the properties of flowfields with a large degree of nonequilibrium are predicted. Nonequilibrium velocities in excess of the equilibrium values are predicted for the initial expansion process. Vibrational nonequilibrium in oxidizer-rich core flows of hydrogen–oxygen rocket engines is then investigated computationally. Vibrational relaxation rate data of oxygen in combustion product gases are obtained from experimental data, empirical correlations, and extensions of available theory. Nonequilibrium flowfield effects are computed and shown to be minor in terms of performance losses caused by relatively rapid vibrational relaxation of oxygen in the product gas mix. Temperature measurements based upon vibrational population are subject to significant error, however. Uncertainty in the relaxation rate of oxygen in water vapor leads to large ranges in computational results.

Nomenclature

c_p = specific heat
E = energy
H = enthalpy
h = Planck constant
k = Boltzmann constant
N = Avogadro constant
p = pressure
Q = heat
R = universal gas constant
s = entropy
T = temperature
U = velocity
θ = characteristic molecular temperature
μ = reduced oscillator mass
ν = molecular vibrational frequency
τ = relaxation time constant
Φ = ratio between compression and expansion relaxation times
χ = mole fraction

Subscripts
TR = translation–rotation
V = vibration
0 = stagnation value

Introduction

THE presence of thermal nonequilibrium in hydrogen–oxygen advanced propulsion systems has been suggested in the past as a possible source of inefficiency. The use of vibrational temperature measurements[1] for comparison with computational fluid dynamic results also necessitates knowledge of the vibrational energy content of the gas relative to an equilibrium state. Herein, the effect of vibrational nonequilibrium on the properties of an expanding gas is modeled. Expanding nitrogen flowfields are investigated because of the availability of experimental data in the form of static pressures and vibrational temperatures. Extensions are then made to the combustion product gas mixture of interest.

Low-thrust hydrogen–oxygen rocket engines frequently combine an oxidizer-rich core with a cooling hydrogen layer flowing along the walls. The core products thus consist mainly of water vapor and oxygen. Molecular oxygen is known to relax relatively slowly in the vibrational modes, raising the possibility of nonequilibrium expansion and inefficiency. Vibrational nonequilibrium would also affect the utility of vibrational population measurements obtained as verification data for computational efforts. Two chambers of interest are examined here: 1) a rectangular chamber that is being tested experimentally under a parallel program and 2) a 30-deg axisymmetric rocket nozzle representative of actual thrusters.

The enthalpy of a gas may be divided into vibrational, rotational, and translational contributions. Expressions for the energy stored in each mode are, for diatomic molecules,[2]

$$H = \tfrac{5}{2}RT \tag{1}$$

$$H = RT \tag{2}$$

$$H = Nh\nu[\exp(h\nu/kT) - 1]^{-1} \tag{3}$$

for the translational, rotational, and vibrational modes, respectively. Referencing computed values to 298.15 K yields the familiar total enthalpy as a function of temperature. For nitrogen at a temperature of 3000 K, the fraction of total internal energy given by translational, rotational, and vibrational components is 61, 24, and 15%, respectively. The question of interest here is whether a gas initially at high temperature and expanding to a low temperature will exhibit significantly altered flowfield properties if the evolving internal energy does not follow the equilibrium distribution specified in Eqs. (1–3); that is, if the three represented temperatures are not equal. Two examples of where such a situation might arise are hypersonic testing utilizing shock tunnels and rocket nozzle flowfields.

Presented as Papers 95-2075 and 95-2076 at the AIAA 30th Thermophysics Conference, San Diego, CA, June 19–22, 1995; received July 20, 1995; revision received June 15, 1996; accepted for publication Oct. 15, 1996.

*Graduate Student; currently Advanced R&D Engineer, BF Goodrich Aerospace, Brecksville, OH 44141. Student Member AIAA.
†Professor. Member AIAA.
‡Active Professor Emeritus. Fellow AIAA.

Both rotational and translational relaxation occur very rapidly, typically requiring only 1–10 collisions per molecule to equilibrate energy levels inconsistent with the overall thermal energy content. Vibrational relaxation, however, can require from 10^3 to 10^8 collisions.[3] Rotational and translational nonequilibrium are typically observed in very low-density flows. Such flows are typically treated through Monte Carlo methods, as in Chung et al.[4] This investigation focuses upon the intermediate range between those very rarified flows and equilibrium conditions. Flows are assumed to have equilibrium between rotational and translational modes with the possibility of significantly nonequilibrium vibrational energy.

Vibrational Relaxation

Energy equilibration occurs principally through collisions between molecules for the conditions of interest here. The difference in rate between vibrational and rotational or translational relaxation lies in the probability of energy transfer per collision. For rotational energy, the quanta of energy involved are quite small, and so transfer is greatly facilitated. Vibrational energy quanta are much larger in general, and only the more energetic collisions are capable of transferring energy between this mode and translational energy. As a result, the time scales involved are much longer, and may be comparable with flowfield time scales under certain conditions. For certain gases, energy transfer may occur through vibrational and rotational modes as well, which can result in more efficient relaxation.

The probability of transfer of vibrational energy per collision is a function of the molecule of interest, the collision partner, and conditions of collision. Vibrational relaxation was studied in the early 1900s in studies of sound propagation and attenuation.[5,6] In the sixties, the initiation of high-enthalpy flight reintroduced the topic.[7,8] The seventies, with the advent of the gasdynamic laser, brought increased studies[9,10] focusing on more complex gas mixtures typical of lasing media. More recently, the high-enthalpy flows of future vehicles have extended interest to temperatures of 40,000 K.[11–13] The work presented herein is tailored to current chemical propulsion systems and deals with a lower temperature range, up through a few thousand Kelvin.

Following the establishment of a considerable database of relaxation times in compression flows, typically obtained through shock-tube experiments, investigations into the relaxation rates in expansion flows revealed discrepancies between the two systems.[14] Expansion flows were frequently observed to relax much more quickly than compression flows. Further complicating the issue was a wide range in reported relaxation times in expansion. Some theoretical works[15,16] attributed the more rapid relaxation to anharmonic effects, while the effect of impurities was suggested as another factor.[17] Anharmonic effects are turned to advantage in the generation of vibrational population inversions for gasdynamic lasers.[9] A discussion of the relationship between anharmonic effects and vibrational relaxation rate is beyond the scope of this article. It is sufficient to note that generically, the presence of anharmonicities tends to result in more rapid relaxation. The discrepancy between compression and expansion relaxation times is usually handled through the introduction of a ratio between the two, as in

$$\Phi = \tau_{\text{compression}}/\tau_{\text{expansion}} \tag{4}$$

The present work utilizes this scheme as well for comparisons with experimental data from expanding nitrogen flowfields. While the probable source and magnitude of Φ and its effects are mentioned, the focus of the investigation is the effect of vibrational nonequilibrium upon the flow properties of pressure, temperature, density, and velocity.

Nitrogen Vibrational Relaxation Time

Millikan and White[18] compiled relaxation rate data and developed an empirical expression relating subject and bath molecule, local temperature (Kelvin) and pressure (atmospheres), and relaxation time as

$$\log_{10}(p\tau) = 5 \times 10^{-4} \times \mu^{1/2} \times \theta^{4/3} \times (T^{-1/3} - 0.015 \times \mu^{1/4}) - 8.0 \tag{5}$$

which is valid for systems wherein vibrational–translational energy transfer is the dominant mechanism. For investigations in nitrogen with nitrogen as the bath molecule, the reduced mass is $\mu = 14$, and the characteristic temperature of vibration is $\theta = 3395$ K. The rate of vibrational energy change is then given by the well-known formula developed by Landau and Teller[19] as

$$\frac{dE_V}{dt} = \frac{E_V(\text{equilibrium}) - E_V}{\tau} \tag{6}$$

using τ as described by various correlations.

Oxygen Vibrational Relaxation Time

The rectangular diagnostic rocket chamber is film cooled by hydrogen flowing along the upper and lower walls. Typically, 75% of the total hydrogen flow is directed to the film cooling. The remainder is injected along with the total oxygen mass flow in the core. A typical test has a core flow mass ratio (MR) of 32, an overall $MR = 8$, and a chamber pressure of approximately 40 psia. Experimental data abound for τ as a function of local temperature and pressure for various gases. Relaxation rates are highly dependent upon the collision partner, or bath molecule. Experimental data have been located for the relaxation rate of molecular oxygen in three of the bath molecules of interest, namely O_2, O, and H_2. Little data have been found for de-excitation resulting from collisions with H_2O, OH, or H. A summary of the experimental data available for appropriate species is now presented, as well as application or extension of existing theoretical frameworks to those bath molecules where little or no data are available.

O_2–O_2

Pure molecular oxygen has been investigated in shock-tube studies, as presented by various authors and compiled by Millikan and White.[18] Their result, presented in Eq. (5), is utilized for oxygen with $\mu = 16$ and $\theta = 2239$ K.

O_2–O

Kiefer and Lutz[20] studied O_2 relaxation in atomic oxygen through shock-wave decomposition of ozone, and found that for a temperature range of 1600–3300 K

$$p\tau = 4.35 \times 10^{-8} - (7.75 \times 10^{-12})T \tag{7}$$

where again p is in atmospheres, T is in Kelvin, and τ is in seconds. The relaxation times given by this empirical fit are two orders of magnitude shorter than those typical of translational–vibrational processes.

O_2–H_2

Data for molecular hydrogen bath relaxation of oxygen were compiled by Millikan and White[18] for shock-tube flows. Their formula as shown in Eq. (5) can be applied with $\theta = 2239$ K and $\mu = 1.88$, yielding relaxation times from one to three orders of magnitude faster than molecular oxygen bath relaxation at relevant temperatures. The high-energy transfer probability results from collisions of oxygen with hydrogen molecules of high thermal velocity.

Theoretical Extensions for Relaxation Rates

Existing analytical results for transfer of vibrational energy through translational, vibrational, and rotational modes were extended in development of relaxation time constants for ox-

ygen in the remaining bath molecules. Each bath specie was examined in the context of energy transfer through each applicable mechanism.

O_2–H_2O

Water vapor is the dominant combustion product and presents the most difficulty in determination of relaxation time. The available experimental data for oxygen in a water vapor bath is limited. Knudsen,[5] Kneser,[6] and Knudsen[21] present experimental investigations and analyses of the effect of water vapor on the absorption of sound in oxygen and air with interpretation in terms of vibrational relaxation efficiencies. Cottrell and McCoubrey[22] conclude that the ratio of transition probabilities for oxygen–water collisions to oxygen–oxygen collisions is approximately 21,000 based on this work. However, extrapolation of their low H_2O concentration data to the mole fractions of interest in the current investigation leads to unrealistic results. Jones et al.[23] present analyses of oxygen relaxation in water vapor based upon the transfer of energy between oxygen vibrational energy and the translational, vibrational, and rotational modes of H_2O, and develop the corresponding analyses for nitrogen in parallel. Vibrational–vibrational energy transfer was found to be the most efficient path for relaxation in the nearly resonant O_2–H_2O system, leading to relaxation times of the order of 10^{-7} s at a pressure of 1 atm. The relaxation time was modeled after the theory of Refs. 24–26 with the result of

$$p\tau = \frac{4.5 \times 10^{-7}[\exp(2.7 \times T^{-0.5}) + \exp(-2.7 \times T^{-0.5})]^2}{\sqrt{T}[1 - \exp[(-2239)/T]]} \tag{8}$$

where T is local translational–rotational temperature in Kelvin and p is in atmospheres.

O_2–OH

No data has been found for oxygen relaxation in a hydroxyl bath. This combustion radical is predicted to be present in significant quantity through an equilibrium CETPC[27] analysis. On a vibrational to translational energy transfer basis, the theory of Millikan and White[18] can be applied with $\mu = 11.10$. Equation (5) is applied as shown previously, again with $\theta = 2239$ K, oxygen being the oscillator of interest. The fundamental vibration of OH is at 3735 wave numbers, quite far from the second harmonic of oxygen at 3160 cm^{-1}, and so vibrational–vibrational energy transfer is expected to be less efficient than in the O_2–H_2O case. This expectation is fulfilled when vibrational–vibrational transfer is calculated through Rapp et al.[24–26] with deduced rates comparable to those resulting from V–T transfer. Application of Moore's[28] rotational–translational energy transfer theory to the O_2–OH system results in relaxation times from one to two orders of magnitude shorter than those resulting from either translational–vibrational transfer or vibrational–vibrational theory. Therefore, R–V transfer is assumed to be the responsible mechanism for relaxation, with a rate represented by

$$p\tau = [1.76 \times 10^{13} \times T^{-2/3} \times \exp(-120 \times T^{-1/3}) \times \exp(1140/T) \times [1 - \exp(-2239/T)]]^{-1} \tag{9}$$

where T is again T_{TR} in Kelvin.

O_2–H

For atomic hydrogen baths, no experimental data have been found. However, no rotational or vibrational transfer mechanisms exist. In the absence of evidence to the contrary, it is assumed that no unusually rapid mechanism such as that operative in the case of O_2–O exists. Thus, Millikan and White's[18] V–T energy transfer formula is applied with a reduced mass of $\mu = 0.97$. The extremely low reduced mass results in a rapid relaxation rate for a V–T mechanism.

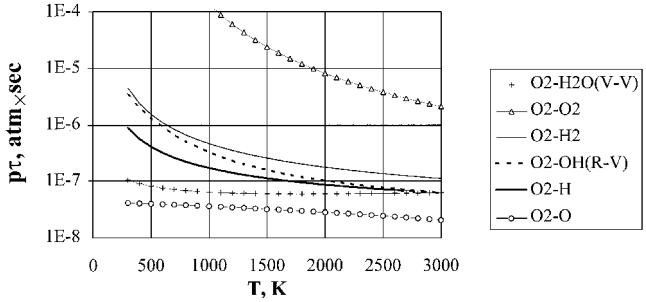

Fig. 1 O_2 relaxation times in H_2–O_2 combustion product gases.

Overall Relaxation Rate

Relaxation times for each bath component are graphically summarized in Fig. 1. The equilibration times vary over orders of magnitude, with all other species providing much more efficient relaxation paths to oxygen molecules than oxygen itself. The various time constants are weighted according to the formula[22]

$$\frac{1}{p\tau} = \sum_{i=1}^{n} \frac{\chi_i}{(p\tau)_i} \tag{10}$$

The presence of bath species other than oxygen results in rapid relaxation relative to that of pure O_2. The impact of the uncertainty in relaxation time will be examined in the results section. The importance of accounting for each species is also addressed. Results are presented for a range of mixture ratios through application of Eq. (10) to an equilibrium combustion product mix.

Numerical Method

Nozzle throat pressure, temperature, and gas molecular weight are estimated from specified reservoir properties with the NASA Lewis CETPC code.[27] Computation with the time-marching scheme begins with an estimated translational–rotational temperature equal to that of the previous time step. Vibrational energy, flow velocity, and density are then computed. A ratio of two pressure computations is utilized along with a convergence criterion to iterate translational temperature. One value is provided by the equation of state. The second may be computed either from an integration of the entropy change of the flowfield or through conservation of momentum. Computational schemes for both entropy change and momentum conservation were developed, with the entropy method found to be more practical.

Some results to be presented are compared to previous numerical work based on the analysis of Stollery and Smith.[29] They presented a numerical method to determine vibrational temperature evolution in a nozzle flow. However, they were not interested in the impact of vibrational nonequilibrium on other flow variables, and so developed a simple method of estimating the vibrational temperatures only. Their analysis showed the effect of other flow variables on vibrational temperature evolution to be minor, and so they did not compute nonequilibrium flow properties. The emphasis in this work is the effect of vibrational nonequilibrium on flowfield properties.

Nozzle flow is computed through a quasi-one-dimensional inviscid flowfield expansion beginning at the throat. The flow is assumed to expand in equilibrium until a Mach number of 1.04 is reached. This is necessary to avoid a change in sonic conditions in the throat region because of energy removal. This delayed onset of nonequilibrium results in negligible differences in the overall energy removed and subsequent effect on the flowfield. Vibrational energy in excess of the equilibrium

value represent energy that, under equilibrium conditions, would be distributed to translational and rotational modes. This excess vibrational energy is effectively a loss of internal energy. As such, nonequilibrium is handled through modeling the excess energy over the equilibrium value as energy removed from the flow in a nonadiabatic expansion. Vibrational relaxation times are calculated locally as the computation progresses down the nozzle, based on local translational temperature and static pressure.

A nozzle flow computation begins with calculation of the vibrational energy through the evolution described in Eq. (6). The equilibrium enthalpy corresponding to the current translational temperature estimate is found through use of the NASA empirical data fits of McBride et al.[30] The vibrational energy corresponding to the translational temperature is computed from Eq. (3). The effective energy loss of the flow is the amount of excess vibrational energy over this translational temperature value. Velocity can be obtained from the total enthalpy, the equilibrium value corresponding to local translation temperature, and the excess vibrational energy through

$$U_{i+1} = [[H_{\text{total}} - H_{\text{TR},j+1} - (E_{V,j+1} - E_{V,\text{TR},j+1})] \times 2]^{1/2} \quad (11)$$

Streamwise distance traveled in the previous time step is given by the product of the velocity and time-step size; nozzle area is calculated from the contour as a function of axial distance. The area, velocity, and mass flow rate are then used to arrive at flow density.

Pressure is first computed from the equation of state utilizing the translational temperature of the molecules. Translational temperature is used because of the origin of pressure in the thermal motion of molecules. A second pressure computation is obtained through integration of the expression

$$\mathrm{d}s = c_p \frac{\mathrm{d}T}{T} - R \frac{\mathrm{d}p}{p} \quad (12)$$

The only restriction placed on the validity of this expression is that the gas is thermally perfect; that is, the gas can be modeled by the equation of state used previously in computation of pressure. It is valid for calorically imperfect gases, necessary for this application because of the variation of specific heat with temperature. The c_p used in the previous expression is the equilibrium value corresponding to the gas translational temperature. The equilibrium value is used because the excess vibrational energy is modeled as heat removed from an equilibrium gas at T_{TR} with a corresponding equilibrium vibrational energy. The specific heat as a function of temperature is provided by McBride et al.[30]

Entropy increase is computed through

$$\mathrm{d}s = \frac{\mathrm{d}Q}{T} \quad (13)$$

where $\mathrm{d}Q$ is the increase in excess energy remaining in the vibrational modes from the previous time step. The integration is performed stepwise and summed as the flow calculation progresses down the nozzle. A ratio of the two expressions for pressure as a function of the estimated temperature is utilized with a Newton–Raphson root-solving method used to arrive at a new translational temperature estimate. Iteration is performed until the ratio of the two pressures is within 10^{-5} of unity, and the solution is marched forward in time. Simulations typically require a few minutes of desktop computer time, depending upon the nozzle length and gas velocity.

Results

Equilibrium Expansion Verification

A computation was first performed for air in vibrational equilibrium, in the ideal gas limit with a specific heat ratio equal to 1.4. Results were compared with the NACA 1135 tabulation[31] for expansion from a nozzle throat to an area ratio of 144. Static pressure, static temperature, and density ratios all agreed with the tabulated data, providing confirmation of equation formulation in the equilibrium limit, where relaxation proceeds extremely rapidly. A similar investigation was conducted for expansion of combustion gases with frozen chemistry and near vibrational equilibrium through comparisons with the NASA Lewis CETPC code[27] operated in rocket nozzle mode. This investigation also confirmed the validity of the code for adiabatic expansions as well as the modeling of the product gas mixture properties.

Nonequilibrium Nitrogen

Data for comparison of computational and experimental nonequilibrium gas pressures were obtained from the experimental investigations of Nagamatsu and Sheer.[8] Nitrogen and air were expanded in a hypersonic shock tunnel through a 30-deg included angle conical nozzle with reservoir pressures of 100, 200, and 500 psia. The stagnation temperature range was approximately 2000–7000 K. The experimental data presented consist of static pressure measurements taken at an area ratio of 144. For the computations presented herein, only diatomic nitrogen was modeled; as such, computations were only performed up to a temperature of 5500 K, where dissociation begins to become significant. The experimental test gas did contain an unspecified level of moisture, introducing uncertainty into the relaxation time of the gas.

Shown in Fig. 2 is an example of the experimental data of Nagamatsu and Sheer[8] at a stagnation pressure of 100 psia. As a check on the code formulation, fully frozen and equilibrium computations were performed, and the results compared with the published analytical results of Nagamatsu and Sheer,[8] with good agreement. The lines on Fig. 2 represent computations performed with varying values of Φ. Increasing values of Φ correspond to more equilibrium expansions, and hence, higher static pressures. The data indicate that vibrational relaxation proceeded at a rate far above that found for the compression case, i.e., $\Phi \gg 1$ for these expansions. The values deduced are actually far above those observed in other experimental investigations.[14] Notably, a large effect of vibrational nonequilibrium on static pressure is observed experimentally and is reproduced computationally. Nonequilibrium lowers the available energy of the flow, decreasing static pressure from the adiabatic, isentropic limit.

There are two likely sources for the decrease in relaxation time, or more equilibrium nature, of the experimental expansions from that predicted by established compression relaxation rate data. Anharmonicities and impurities are both capable of causing this decrease. Various investigations have been made into the effect of water vapor on nitrogen relaxation times.[5,22,32,33] Huber and Kantrowitz[32] obtained experimental data showing an order of magnitude decrease in relaxation time for nitrogen with water vapor concentrations of ~1%. Russo[33] found that a concentration of 0.1% resulted in a noticeable decrease in relaxation time. Knudsen,[5] however, con-

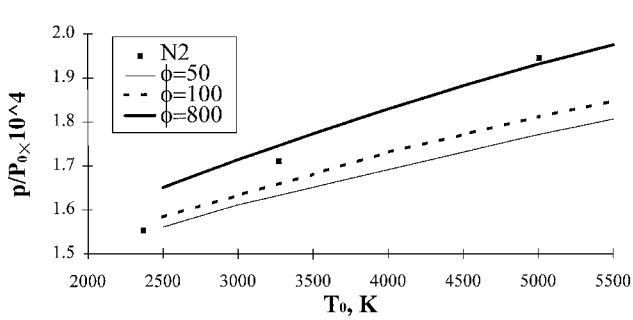

Fig. 2 Nondimensional static pressures[8] and current computations; N_2, P_0 = 100 psia.

cluded that humidity has no effect on the relaxation rate of nitrogen. The review by Cottrell and McCoubrey[22] shows the majority of the available data agreeing on the significant effect of water vapor presence on nitrogen vibrational relaxation. Based on the work of Huber and Kantrowitz[32] and Cottrell and McCoubrey[22] a vapor concentration of the order of 2% is required to reduce the nitrogen relaxation time by a factor of 50. With the much higher values of Φ indicated here, it appears that a mechanism other than that of water vapor contamination may be responsible. In light of the extremely rapid expansion conditions, it is possible that anharmonic effects[15,16] also come into play in the highly nonequilibrium flow observed.

A second source of nonequilibrium nitrogen expansion data are temperature measurements by Hurle et al.[34] Line reversal techniques were utilized in a 15-deg included angle nozzle expansion to measure vibrational temperatures. A shock tube was used to generate the reservoir conditions in a manner similar to the method of Nagamatsu et al.[7,8] The primary conclusion drawn by Hurle et al.[34] was that nitrogen relaxation in the flowfield proceeded with a rate 15 times that present in compression flows. Their computational work was based upon that of Stollery and Smith.[29] Using a parabolic throat geometry as an approximation for the unspecified initial nozzle contour and a 15-deg included angle conical nozzle, numerical solutions to Hurle et al.'s[34] experiments were obtained.

Comparisons with the experimental data indicate a value for Φ of 70 at AR = 8, and 140 at AR = 32.[35] The discrepancy between this result and Hurle et al.'s[34] quoted value of $\Phi = 15$ is because of differences between the compression relaxation rate data used. Regardless of the shock wave relaxation data used, it is clear that relaxation rates more rapid than those observed in compression flows are observed in both the data of Nagamatsu and Sheer[8] and Hurle et al.[34] The striking temperature dependence displayed in the data of Nagamatsu et al.[8] was not observed. Hurle et al.[34] concluded that the observed rapid relaxation was not caused by the presence of impurities or experimental error.

A recent series of papers[36–38] has reported on the utilization of spontaneous Raman spectroscopy in an investigation of nitrogen vibrational relaxation in nozzle flows generated by a shock tunnel. The conclusion reached by these investigators was that Φ has a value very close to 1; that is, nitrogen relaxes at nearly the same rate whether in an expansion or compression flow. Their stagnation conditions were a pressure of 102 atm and a temperature of 2800 K. Computations with Φ values between 1–5 bracket the experimental data. The extremely rapid de-excitation observed by Nagamatsu et al.[7,8] and Hurle[34] is not observed here. These measurements were made at small area ratios of approximately 3 and 5.5.

A limitation of the computational results discussed is the assignment of one effective Φ value applied throughout the expansion. It is notable that among the data modeled, those obtained at larger area ratios required correspondingly larger effective Φ values for simulation. The computation of exchange rates throughout the expansion process, as in Bray,[15] Treanor et al.,[16] and Sharma et al.,[36] for example, is indicated to be more physically correct than assumption of a value of Φ, as pointed out by Gillespie et al.[37] Unfortunately, a solution of vibrational exchange equations is more computationally intensive. The qualitative agreement presented previously provides confidence in the mathematical formulation of the nonequilibrium thermodynamics. Flowfield effects as a function of degree of nonequilibrium for expanding nitrogen are now discussed, followed by extension to hydrogen–oxygen combustion products.

Effect of Initial Nozzle Contour

A brief investigation into the importance of the initial nozzle contour was conducted for the 15-deg nozzle of Hurle et al.[34] because of the unspecified throat contour. Differences in vibrational temperature between an assumed parabolic contour and a strictly conical nozzle were found to be minor for the conditions simulated, and no significant differences in flow properties were observed. However, in general, initial nozzle contour can affect the flowfield downstream. There are three possible flow regimes: 1) severe initial nonequilibrium, where the energy removed is significant regardless of initial contour; 2) near equilibrium flow, where sufficient collisions occur regardless of the initial expansion rate; and 3) nonequilibrium between the above two limits, where a smooth contour allows near-equilibrium expansion, but a sharp initial expansion results in significant energy removal. The characteristics exhibited by a particular flowfield depend upon nozzle contour, collision frequency, and transition probability.

Flowfield Effect of Nonequilibrium

The effect of relaxation time on the expansion of nitrogen in a 30-deg included angle conical nozzle with a parabolic throat was studied to observe changes in flowfield characteristics for conditions ranging from equilibrium to vibrationally frozen. The experimental results of Nagamatsu and Sheer[8] indicate a significant effect of vibrational nonequilibrium upon static pressure. The numerical results presented indicate nonnegligible flowfield effects as well. To investigate further, stagnation conditions representative of the small rocket engines of interest were chosen, with a reservoir pressure and temperature of 40 psia and 3000 K. To investigate the effect of the degree of nonequilibrium, Φ was varied from 1 to 10^7, corresponding to flows ranging from fully frozen to nearly equilibrium. Results are presented for nitrogen expanding to an area ratio of 32 in Figs. 3 and 4. Figure 3 displays vibrational and translational–rotational temperatures as a function of Φ, useful in visualization of the degree of nonequilibrium in a flowfield. For Φ between 1–10, the flow is essentially frozen at the throat condition. As Φ approaches 10^7, the flow is nearly in equilibrium, and the temperatures approach one another. The variation in T_{TR} is much smaller than that in T_V because of a relatively small change in energy. Figure 4 displays the effect of nonequilibrium on translational–rotational temperature, pressure, and velocity at an area ratio of 32. Values are presented as a percentage of the equilibrium value, again as a function of Φ. Highly nonequilibrium flows exhibit large drops in static pressure and temperature, of the order of 25% for this

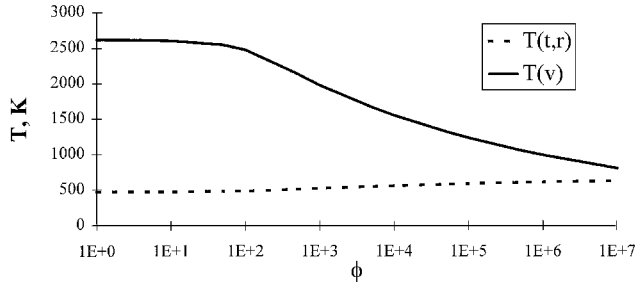

Fig. 3 Vibrational and translational–rotational temperatures as a function of Φ.

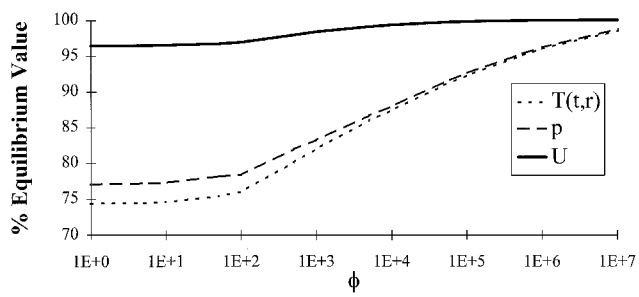

Fig. 4 Translational–rotational temperature, static pressure, and velocity as a function of Φ; AR = 32.

condition. Note that the temperature and pressure, for a given degree of nonequilibrium, exhibit nearly the same decrease. As such, the density effects are expected to be small in comparison. Since temperatures are low relative to pressures, an increase in nonequilibrium density is indicated, which is demonstrated by the decrease in velocity. As indicated by the small difference between the temperature and pressure losses, the magnitude is smaller, with a maximum loss of approximately 3.5% in exit velocity.

An interesting result is obtained in the beginning portion of the nozzle expansion, where velocity is observed to increase relative to an equilibrium expansion. This result is consistent with a nonadiabatic cooling pipe flow of a supersonic gas, where velocity is expected to increase, while temperature, density, and pressure decrease. As the gas progresses down the nozzle, the expansion converts internal energy to kinetic energy. The decreased availability of internal energy because of nonequilibrium results in lower kinetic energy, and the flow velocity is less than in the equilibrium case.

H_2–O_2 Rocket Rectangular Diagnostic Chamber

Using the previous relaxation times for molecular oxygen, the nonequilibrium flowfield was computed for the diagnostic chamber of interest, which will be referred to as the rectangular chamber throughout this text. The combustion chamber is square in cross section, 2.54 cm on each side. The sidewalls are parallel throughout the rocket. Following a 5.08-cm-long straight section, the upper and lower walls converge with a 30-deg half-angle to a throat height of 0.635 cm. The upper and lower walls then diverge with a 15-deg half-angle to an exit area ratio of 8. Figure 5 shows the computed discrepancy between translational–rotational and vibrational temperatures in Kelvin. This quantity is of interest because of the use of vibrational Raman temperature measurements as a flowfield diagnostic. Results in a parallel experimental investigation[39,40] indicate an extremely oxygen-rich flow along the rocket centerline. Thus, results are presented for a mixture ratio of 100. These data indicate the expected error when measuring vibrational temperature and assuming equilibrium between the vibrational and translational modes. According to baseline estimates, the vibrational and translational temperatures should be within tens of Kelvin throughout the nozzle. Nonequilibrium effects are thus predicted to be relatively minor for the slowly expanding diagnostic rocket chamber.

Considerable uncertainty exists in the vibrational relaxation time of oxygen in some of the various bath gases. The derived relaxation times utilized should only be considered order of magnitude estimates. Thus, Fig. 5 also includes the range of temperature difference between vibrational and translational–rotational modes for the derived relaxation time scaled up and down by an order of magnitude. This is also instructive in light of the ambiguities concerning both mixing effectiveness and possible anharmonic effects. The resulting range in computed temperature difference is very large, ranging from near equilibrium to discrepancies of hundreds of Kelvin at the rocket exit. While baseline estimates indicate that vibrational measurements should be valid, cognizance of the limitations of the relaxation rate data prohibits the assumption of equilibrium in the nozzle. The sharp initial development of nonequilibrium in the near-throat region is not followed by a return to equilibrium for the slower relaxation bound. Energy transfer is of sufficiently low probability that the degree of nonequilibrium increases monotonically throughout the rocket nozzle.

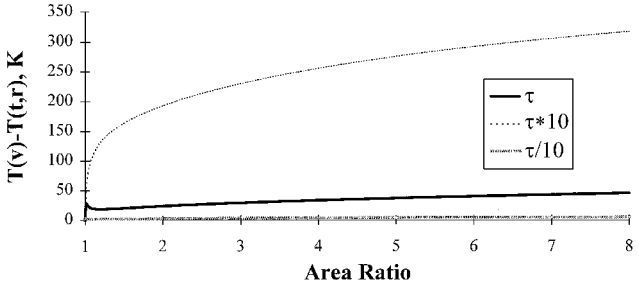

Fig. 5 Effect of order of magnitude change in relaxation time on temperature discrepancy.

Conical Nozzle

Results for a 30-deg conical nozzle are now presented to illustrate the possible magnitude of inefficiency for a typical thruster as a function of mixture ratio and area ratio, for the same stagnation temperature and pressure as examined with the rectangular chamber. A parabolic throat is mated to a conical nozzle for these simulations. Figure 6 shows the discrepancy between translational and vibrational temperatures. The discrepancy is larger than for the rectangular chamber at a given area ratio except in the throat region, where the sharp cornered nozzle considered previously provided an extremely rapid initial expansion. Large differences exist between vibrational and translational temperatures in the downstream region. Increasing oxygen concentration at higher *MR* flows results in more severe nonequilibrium.

In Fig. 7, the computed nonequilibrium temperature, pressure, density, and velocity are shown as a percentage of their respective equilibrium values for $MR = 100$. While the losses are perhaps an order of magnitude larger than present in the slowly expanding rectangular chamber, they are still rather minor, with a 1.5% decrease in static pressure and translational temperature at maximum. Velocity loss is only expected to be of the order of 0.5% at the rocket exit relative to an equilibrium expansion. It is interesting to note the differences between the conical nozzle nonequilibrium flowfield and that of the rectangular chamber. The smooth parabolic throat contour of the 30-deg rocket nozzle allows more time for the vibrational energy to adjust to flowfield conditions during the initial period of rapidly dropping thermal energy. The overall more rapid expansion of the conical rocket nozzle leads to more significant nonequilibrium effects further down the nozzle, however. While the effects of nonequilibrium are more significant than for the slowly expanding rectangular chamber, effects are still much smaller than in an expanding diatomic gas

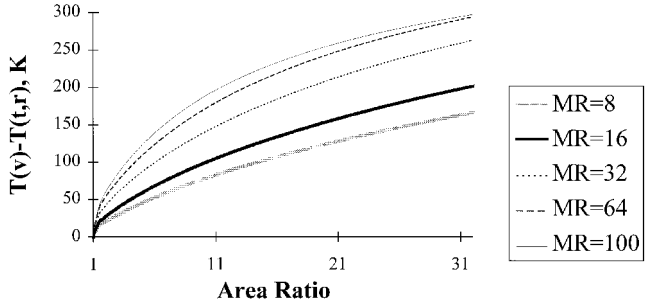

Fig. 6 Discrepancy between vibrational and translational temperatures in conical nozzle.

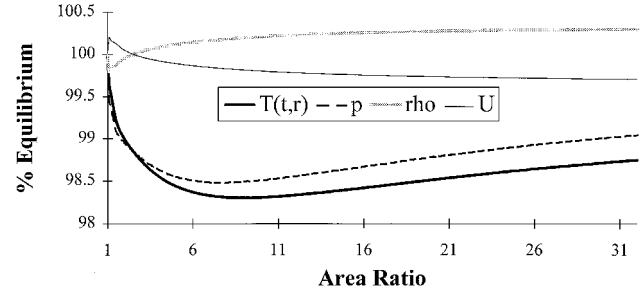

Fig. 7 Temperature, pressure, density, and velocity as percent of equilibrium in conical nozzle.

due to the rapid relaxation paths provided by the combustion products.

The return to equilibrium of flowfield properties occurs with the release of excess vibrational energy to the other modes. The discrepancy between vibrational energy content and the equilibrium value is indicated by the temperature and pressure curves. During the initial rapid expansion, rapidly increasing nonequilibrium removes internal energy from the flow, thus increasing the discrepancy between equilibrium temperature and pressure values and the corresponding nonequilibrium flowfield properties. After the vibrational relaxation rate catches up to the rate of change of internal energy, temperature and pressure begin to return to equilibrium. Temperature and pressure do not return at the same rate, however, preventing the restoration of velocity and density to equilibrium values.

As noted, there is considerable uncertainty in the relaxation time of molecular oxygen in several of the bath gases, most importantly water vapor. The most severe nonequilibrium effects are expected in the conical rocket nozzle with a oxidizer-rich environment. Increasing relaxation time by a factor of 10 results in nonequilibrium profiles similar to those shown in Fig. 7, but with larger departures from the equilibrium values. Temperature and static pressure drop to approximately 92% of their equilibrium values before the rocket nozzle exit is reached. There is a 2% drop in velocity at the nozzle exit, which would proportionately impact thrust. However, there are mitigating factors affecting conclusions regarding adverse performance effects. First, this worst-case scenario only exists on the rocket centerline. Progressing from the engine centerline to the outer wall, a radially varying mixture ratio is expected. Moving toward the hydrogen cooling layer, a progressively more fuel-rich mixture is encountered. This will decrease nonequilibrium by decreasing overall oxygen concentration and by reducing the relaxation time of that present. However, the attendant rise in temperature will increase vibrational energy, offsetting the decrease caused by reduction in number density. Actual performance effects would have to integrate the nonequilibrium flowfield impact across the nozzle exit. Noting that effects are relatively minor except for in the most severe cases of poor mixing, it is likely that the performance losses caused by vibrational nonequilibrium can be considered negligible. However, the relatively large discrepancy between vibrational and translational–rotational temperatures could result in large error in temperature determinations based upon vibrational populations.

The importance of accounting for the minor species in the flow, namely O, H_2, and H, was briefly investigated. Results computed with and without the minor species' contributions to relaxation time show that they do indeed affect computed results significantly. However, their contribution to overall relaxation rate lies within the order of magnitude accuracy of these estimations. Thus, their inclusion is not necessary until more definitive data are developed.

With the limited relaxation rate data available for oxygen in water vapor, it is difficult to make unequivocal statements regarding the effect of vibrational nonequilibrium on thrust production of H_2–O_2 systems. However, it appears likely that flowfield effects are quite small. More generally, it is likely safe to assume that for any of the conventional chemical systems where water is a combustion product, vibrational nonequilibrium is not a significant source of loss. This would be especially true in systems wherein the well-mixed complete combustion desired is more closely attained. The efficient relaxation paths afforded by the water molecule lead to expansions with vibrational modes nearly in equilibrium with kinetic and rotational energies. Temperature measurements based upon vibrational Raman spectroscopy in expanding systems, especially those in an oxidizer-rich area, however, must be viewed with caution.

Conclusions

A computational code for simulation of nozzle gas flows in vibrational nonequilibrium is presented. The code is shown to reproduce experimentally observed effects of nonequilibrium on flowfield properties. The ratio between compression and expansion relaxation times for nitrogen is concluded to be significantly greater than unity at large expansion ratios under certain conditions. Experimental data indicate that this ratio cannot always be accurately represented by a single value throughout the expansion process. Initial nozzle contour can significantly affect the downstream flowfield, depending upon the degree of nonequilibrium present. Flows with significant vibrational nonequilibrium can exhibit large drops in translational–rotational temperature and static pressure, with attendant losses in velocity. Nonequilibrium velocities are predicted to exceed equilibrium values in the initial expansion process.

Estimates of the vibrational relaxation rates of molecular oxygen in various gases are applied to a computational analysis of expanding H_2–O_2 combustion products. Because of the large uncertainty in relaxation time, a wide range of computed results is seen, from nearly equilibrium to significant nonequilibrium. For temperature measurements based upon vibrational energy distribution, large errors are possible because of discrepancies between vibrational and translational temperature in the rectangular test rocket of interest. For this chamber, thrust and pressure losses are not significant. For a representative 30-deg conical nozzle, velocity losses associated with vibrational nonequilibrium in an oxidizer-rich core flow are expected to be between 0–2% at an area ratio of 32. Static pressure decreases at the nozzle exit are expected to range from 0 to 8%. Large discrepancies may exist between vibrational and kinetic temperatures.

Acknowledgments

This work was supported by NASA Grant NGT-51049 under administration of the Graduate Student Researcher Program. R. A. J. is indebted to NASA Lewis Research Center for support of this research. The authors express gratitude to Bonnie McBride for the equilibrium thermodynamic data.

References

[1]De Groot, W. A., and Weiss, J. M., "Species and Temperature Measurement in H_2/O_2 Rocket Flow Fields by Means of Raman Scattering Diagnostics," NASA CR-189217; also, AIAA Paper 92-3353, 1992.

[2]Hirschfelder, J. O., Curtiss, C. F., and Bird, R. B., "Molecular Theory of Gases and Liquids," Structure of Matter Series, Univ. of Wisconsin Naval Research Lab., Madison, WI, April 1963.

[3]Rich, J. W., and Treanor, C. E., "Vibrational Relaxation in Gas-Dynamic Flows," *Annual Review of Fluid Mechanics*, Vol. 2, 1970, pp. 355–396.

[4]Chung, C. H., DeWitt, K. J., Stubbs, R. M., and Penko, P. F., "Simulation of Low-Density Nozzle Plumes in Non-Zero Ambient Pressures," AIAA Paper 94-0357, Jan. 1994.

[5]Knudsen, V. O., "The Absorption of Sound in Air, in Oxygen, and in Nitrogen—Effects of Humidity and Temperature," *Journal of the Acoustical Society of America*, Vol. 5, Oct. 1933, pp. 112–121.

[6]Kneser, H. O., "The Interpretation of the Anomalous Sound-Absorption in Air and Oxygen in Terms of Molecular Collisions," *Journal of the Acoustical Society of America*, Vol. 5, Oct. 1933, pp. 122–126.

[7]Nagamatsu, H. T., Workman, J. B., and Sheer, R. E., Jr., "Hypersonic Nozzle Expansion of Air with Atom Recombination Present," *Journal of the Aeronautical Sciences*, Vol. 28, No. 11, 1961, pp. 832–837.

[8]Nagamatsu, H. T., and Sheer, R. E., Jr., "Vibrational Relaxation and Recombination of Nitrogen and Air in Hypersonic Nozzle Flows," *AIAA Journal*, Vol. 3, No. 8, 1965, pp. 1386–1391.

[9]McKenzie, R. L., "Diatomic Gasdynamic Lasers," *Physics of Fluids*, Vol. 15, No. 12, 1972, pp. 2163–2173.

[10]Taylor, R. L., and Bitterman, S., "Vibrational Energy Transfer in the CO_2-N_2-H_2O Molecular System," *Proceedings of the 7th International Shock Tube Symposium*, Univ. of Toronto Press, Toronto, ON, Canada, June 1969, pp. 577–590.

[11]Hansen, C. F., "Vibrational Relaxation in Very High Temperature Nitrogen," AIAA Paper 91-0465, Jan. 1991.

[12]Gonzales, D. A., and Varghese, P. L., "Vibrational Relaxation and Dissociation in Nitrogen," AIAA Paper 91-1370, June 1991.

[13]Park, C., "Estimation of Excitation Energy of Diatomic Molecules in Expanding Nonequilibrium Flows," AIAA Paper 92-0805, Jan. 1992.

[14]Hurle, I. R., "Nonequilibrium Flows with Special Reference to the Nozzle-Flow Problem," *Proceedings of the 8th International Shock Tube Symposium*, 1971, pp. 3/1–3/37.

[15]Bray, K. N. C., "Vibrational Relaxation of Anharmonic Oscillator Molecules: Relaxation Under Isothermal Conditions," *J. Phys. B (Proc. Phys. Soc.)*, Ser. 2, Vol. 1, 1968, pp. 705–717.

[16]Treanor, C. E., Rich, J. W., and Rehm, R. G., "Vibrational Relaxation of Anharmonic Oscillators with Exchange-Dominated Collisions," *Journal of Chemical Physics*, Vol. 48, No. 4, 1968, pp. 1798–1807.

[17]Russo, A. L., "Importance of Impurities on Vibrational Relaxation Measurements in N_2," *Journal of Chemical Physics*, Vol. 44, 1966, pp. 1305, 1306.

[18]Millikan, R. C., and White, D. R., "Systematics of Vibrational Relaxation," *Journal of Chemical Physics*, Vol. 39, No. 12, 1963, pp. 3209–3213.

[19]Landau, Von L., and Teller, E., "Zur Theorie Der Schalldispersion," *Physikalische Zeitschrift der Sowjetunion*, Vol. 10, No. 34, 1936, pp. 34–43.

[20]Kiefer, J. H., and Lutz, R. W., "The Effect of Oxygen Atoms on the Vibrational Relaxation of Oxygen," *Proceedings of the 11th Symposium (International) on Combustion*, The Combustion Inst., Pittsburgh, PA, 1967, pp. 67–76.

[21]Knudsen, V. O., "The Absorption of Sound in Gases," *Journal of the Acoustical Society of America*, Vol. 6, April 1935, pp. 199–204.

[22]Cottrell, T. L., and McCoubrey, J. C., *Molecular Energy Transfer in Gases*, Butterworths, London, 1961.

[23]Jones, R. A., Myrabo, L. N., and Nagamatsu, H. T., "A Numerical Investigation of the Effect of Vibrational Nonequilibrium in H_2O_2 Rocket Engines," AIAA Paper 95-2075, June 1995.

[24]Rapp, D., and Sharp, T. E., "Vibrational Energy Transfer in Molecular Collisions Involving Large Transition Probabilities," *Journal of Chemical Physics*, Vol. 38, No. 11, 1963, pp. 2641–2648.

[25]Rapp, D., and Englander-Golden, P., "Resonant and Near-Resonant Vibrational-Vibrational Energy Transfer Between Molecules in Collision," *Journal of Chemical Physics*, Vol. 40, No. 2, 1964, pp. 573–575; also "Erratum," *Journal of Chemical Physics*, Vol. 40, No. 10, 1964, pp. 3120–3121.

[26]Rapp, D., "Interchange of Vibrational Energy Between Molecules in Collisions," *Journal of Chemical Physics*, Vol. 43, No. 1, 1965, pp. 316, 317.

[27]Gordon, S., and McBride, B. J., "Computer Program for Calculation of Complex Chemical Equilibrium Compositions, Rocket Performance, Incident and Reflected Shocks, and Chapman-Jouget Detonations," NASA SP-273, March 1976.

[28]Moore, C. B., "Vibration-Rotation Energy Transfer," *Journal of Chemical Physics*, Vol. 43, No. 9, 1965, pp. 2979–2986.

[29]Stollery, J. L., and Smith, J. E., "A Note on the Variation of Vibrational Temperature Along a Nozzle," *Journal of Fluid Mechanics*, Vol. 13, pp. 225–236.

[30]McBride, B. J., Gordon, S., and Reno, M. A., "Thermodynamic Data for Fifty Reference Elements," NASA TP-3287, Jan. 1993.

[31]Ames Research Staff, "Equations, Tables, and Charts for Compressible Flow," Rept. 1135, National Advisory Committee for Aeronautics.

[32]Huber, P. W., and Kantrowitz, A., "Heat-Capacity Lag Measurements in Various Gases," *Journal of Chemical Physics*, Vol. 15, No. 5, 1947, pp. 275–284.

[33]Russo, A. L., "Importance of Impurities on Vibrational Relaxation Measurements in N2," *Journal of Chemical Physics*, Vol. 44, 1966, pp. 1305, 1306.

[34]Hurle, I. R., Russo, A. L., and Hall, J. G., "Spectroscopic Studies of Vibrational Nonequilibrium in Supersonic Nozzle Flows," *Journal of Chemical Physics*, Vol. 40, No. 8, 1964, pp. 2076–2089.

[35]Jones, R. A., Myrabo, L. N., and Nagamatsu, H. T., "A Numerical Investigation of the Effect of Vibrational Nonequilibrium in Expanding Flows," AIAA Paper 95-2076, June 1995.

[36]Sharma, S. P., Ruffin, S., Meyer, S. A., Gillespie, W. D., and Yates, L. A., "Density Measurements in an Expanding Flow Using Holographic Interferometry," AIAA Paper 92-0809, Jan. 1992.

[37]Gillespie, W. D., Bershader, D., Sharma, S. P., and Ruffin, S. M., "Raman Scattering Measurements of Vibrational and Rotational Distributions in Expanding Nitrogen," AIAA Paper 93-0274, Jan. 1993.

[38]Sharma, S. P., Ruffin, S. M., Gillespie, W. D., and Meyer, S. A., "Nonequilibrium Vibrational Population Measurements in an Expanding Flow Using Spontaneous Raman Spectroscopy," AIAA Paper 92-2855, July 1992.

[39]Jones, R. A., Myrabo, L. N., Nagamatsu, H. T., and De Groot, W. A., "Experimental Investigation of Vibrational Nonequilibrium in H_2-O_2 Rocket Engines," AIAA Paper 96-0228, Jan. 1996.

[40]Jones, R. A., Myrabo, L. N., Nagamatsu, H. T., and De Groot, W. A., "Oxygen Temperature and Concentration Measurements in H_2-O_2 Rocket Engines," AIAA Paper 96-0439, Jan. 1996.